tured silica shell (Fig. 4c), which when thermally treated gives rise to mesoporous nanoparticles with radial channels.

The uniform fragment length within the interior of the nanoparticles can be explained by the radial nature of the deformation field around each defect, or site-specific breakage of the 300 nm long native TMV rods. Indeed, chemical degradation of TMV does produce a stable fragment about 50 nm in length,[24] which is similar in size to those encapsulated in the silica shell of the nanoparticles. However, we observed only a random distribution of particle lengths in control samples containing broken TMV tubes. Further work is in progress to confirm the model.

In conclusion, nematic liquid crystals of TMV can be used to prepare silica mesostructures and nanoparticles with parallel or radial arrays of linear channels, respectively. The mesostructures are produced as micrometer-size inverse replicas of the nematic phase, and have a periodicity of approximately 20 nm, which is larger than that generally attainable by current methods. In contrast, the nanoparticles are less than 150 nm in size and consist of a dense silica core surrounded by an unusual radial array of mineralized TMV fragments, 50 nm in length. The channeled nanoparticles are produced at lower reactant concentrations and appear to originate from topological defects associated with the deformation and fracturing of silica–TMV clusters as the liquid crystalline state is re-established in the reaction mixture. The general stability of TMV liquid crystals suggests that it should be possible to use a similar approach to prepare a wide range of inorganic oxides, semiconductors and metal-based mesophases and nanoparticles with mesostructured interiors.

Experimental

TMV liquid crystals were prepared in a nuclear magnetic resonance (NMR) tube using 200 µL of a 16 mg mL^{-1} buffered aqueous suspension of the virus particles. The tube was left for 1 h to give a birefringent viscous gel and 120 µL of a mixture containing 90 mol-% TEOS and 10 mol-% APTES was then added, and the tube agitated gently to mix the two components. The tube was placed in an upright position, and the sample aged for 4 days at room temperature. After this time, the tube was placed in a water bath at 45 °C for 48 h to increase the degree of silica condensation. The resulting white gel was removed from the tube and dried at room temperature overnight. Experiments were also undertaken in the presence of TEOS with 5 and 0 mol-% APTES, and at a constant molar ratio of TEOS/APTES = 9:1 but using 60 % or 30 % of the original volume of organosilane mixture (72 and 36 µL, respectively, to 200 µL of a 16 mg mL^{-1} gel of TMV particles).

Inorganic replicas were prepared by removing the virus from the silica framework on heating to 540 °C at a rate of 1 °C min^{-1}. TGA of the silica–TMV mesostructure showed various stages of weight decrease including; loss of adsorbed water (20 to 180 °C, 15.9 wt.-%,), thermal decomposition of TMV template and amino-propyl moieties (180 to 430 °C, 17.2 wt.-%, and release of water during thermal condensation of the silica framework (430 to 800 °C, 10.6 wt.-%).

Samples for TEM were ground in a mortar and pestle, re-suspended in water, and droplets air-dried onto formvar-covered, carbon-coated copper EM grids. Samples were examined by FTIR spectroscopy using Nujol mulls.

Received: November 21, 2000
Final version: January 26, 2001

---

[1] U. Ciesla, F. Schuth, *Microporous Mesoporous Mater.* **1999**, *27*, 131.
[2] T. J. Barton, L. M. Bull, W. G. Klemperer, D. A. Loy, B. McEnaney, M. Misosno, P. A. Monson, G. Pez, G. W. Scherer, J. C. Vartuli, O. M. Yaghi, *Chem. Mater.* **1999**, *11*, 2633.
[3] G. A. Ozin, *Adv. Mater.* **1992**, *4*, 612.
[4] A. N. Shipway, E. Katz, I. Willner, *Chem. Phys. Chem.* **2000**, *1*, 18.
[5] C. T. Kresge, M. E. Leonowicz, W. J. Roth, J. C. Vartuli, J. S. Beck, *Nature* **1992**, *359*, 710.
[6] G. S. Attard, J. C. Glyde, C. G. Göltner, *Nature* **1995**, *378*, 366.
[7] Y. Lu, H. Fan, A. Stump, T. L. Ward, T. Rieker, C. J. Brinker, *Nature* **1999**, *398*, 223.
[8] C. E. Fowler, D. Khushalani, B. Lebeau, S. Mann, *Adv. Mater.* **2001**, *13*, 649.
[9] D. D. Archibald, S. Mann, *Nature* **1993**, *364*, 430.
[10] J. Coffer, S. Bigham, X. Li, R. Pinnizzotto, Y. Rho, R. Pirtle, I. Pirtle, *Appl. Phys. Lett.* **1996**, *69*, 3851.
[11] W. Shenton, T. Douglas, M. Young, G. Stubbs, S. Mann, *Adv. Mater.* **1999**, *11*, 253.
[12] E. Braun, Y. Eichen, U. Sivan, G. Ben-Yoseph, *Nature* **1998**, *391*, 775.
[13] K. Wong, T. Douglas, S. Gider, D. D. Awschalom, S. Mann, *Chem. Mater.* **1998**, *10*, 279.
[14] T. Douglas, M. Young, *Nature* **1998**, *393*, 152.
[15] A. P. Alivisatos, K. P. Johnsson, X. Peng, T. E. Wilson, C. J. Loweth, M. P. Bruchez, P. G. Schultz, *Nature* **1996**, *382*, 609.
[16] C. A. Mirkin, R. L. Letsinger, R. C. Mucic, J. J. Storhoff, *Nature* **1996**, *382*, 607.
[17] W. Shenton, D. Pum, U. B. Sleytr, S. Mann, *Nature* **1997**, *389*, 585.
[18] S. Mann, W. Shenton, M. Li, S. Connolly, D. Fitzmaurice, *Adv. Mater.* **2000**, *12*, 147.
[19] S. A. Davis, S. L. Burkett, N. H. Mendelson, S. Mann, *Nature* **1997**, *385*, 440.
[20] B.-J. Zhang, S. A. Davis, N. H. Mendelson, S. Mann, *Chem. Commun.* **2000**, 781.
[21] J. D. Watson, *Biochim. Biophys. Acta* **1954**, *13*, 10.
[22] J. Gregory, K. C. Holmes, *J. Mol. Biol.* **1965**, *13*, 796.
[23] J. D. Bernal, I. J. Fankuchen, *J. Gen. Physiol.* **1941**, *25*, 111.
[24] R. N. Perham, T. M. A. Wilson, *Virology* **1978**, *84*, 293.

Electrophoretic Growth of Lead Zirconate Titanate Nanorods**

By *Steven J. Limmer*, *Seana Seraji*, *Mike J. Forbess*, *Yun Wu*, *Tammy P. Chou*, *Carolyn Nguyen*, and *Guozhong Cao**

The synthesis of nano-sized materials has been a very active research area over the past few years, for a variety of reasons. For instance, some materials show markedly different properties when their size is suitably constrained, and nano-sized materials give scientists an opportunity to analyze many quantum phenomena, which were not available for study previously. In addition, the process of miniaturization is important in itself, in both the microelectronics industries, as well as in the development of micro electromechanical systems (MEMS). A number of different techniques exist for the formation of various nanostructures. For instance, small nanoparticles, or quantum dots, have been fabricated by using micelles as miniature reactors, in which the reactions are carried out, yielding fairly monodisperse particles.[1] Films on the order of less than one nanometer to a few nanometers thick have been fabricated by using self-assembled monolayers.[2]

---

[*] Prof. G. Z. Cao, S. J. Limmer, S. Seraji, M. J. Forbess, Dr. Y. Wu,
T. P. Chou, C. Nguyen
Department of Materials Science and Engineering
University of Washington
Seattle, WA (USA)
E-mail: gzcao@u.washington.edu

[**] The authors thank PNNL (S. J. Limmer), Ford Motor Co. and the Center for Nanotechnology at the University of Washington (S. Seraji), and the NSF IGERT fellowship (Y. Wu and S. J. Limmer) for financial support.

One of the most common techniques used for the formation of certain nano-sized structures (such as rods, wires, and hollow tubules) is template-based synthesis, in which the desired materials are grown within the pores of a porous membrane (such as track-etched polycarbonate (PC) or anodic alumina). This technique has been widely used to form numerous materials, including metal and polymer nanorods,[3–6] oxide nanorods,[3,4,7,8] and composite nanostructures.[3,9] For the template formation of oxide nanorods, two main techniques are used. The first involves a two-step process. Using electrochemical methods, metal wires are grown in the template (the same technique used to form metal nanorods). Then, the metal wires are oxidized, either electrochemically or by heating them in air, to form the oxide nanorods.[8] The other method has been to use sol–gel processes to directly fill the template with the desired oxide, which is then crystallized by heating.[3,7] Both approaches have limitations, however. For instance, it is very difficult to make complex metal oxides with the first method. While mixed-metal nanostructures have been made,[5] they are generally comprised of discrete layers, rather than being homogeneously distributed. Thus, there is no guarantee that oxidizing them would directly result in an oxide compound of the desired stoichiometry and crystal structure. Since complex oxides comprise so many important and interesting materials (e.g., ferroelectrics, piezoelectrics, conducting oxides, and magnetic materials), a method to grow complex oxide nanorods would be of great interest.

Direct sol filling can also be used to grow nanorods. For instance, nanorods of TiO_2 have been grown by immersing a template membrane in a titania sol.[3,7] However, there are some potential limitations to this technique. The main drawback is that capillary action is the only driving force to form nanorods from the sol. Also, sols commonly have a very low solids content (~5 vol.-%), so that even if the pores are filled with sol, the packing of solids in the pores is very low. Increasing the concentration of the sol could help this somewhat, but raising the concentration too high would result in either a sol so viscous that filling of the pores would be difficult, or destabilization of the sol. Thus, the packing of material within the pore is likely to be significantly less than the maximum possible density. This could potentially lead to cracking and defects caused by the large volume change upon drying as the solvent is removed. In addition, the degree of shrinkage will be very high, leading to nanorods that do not have the shape and dimensions of the template used, or are hollow tubes. One technique that might overcome these limitations is the electrophoretic sol–gel method, in which an applied electric field induces electrophoretic motion of the nanoclusters in the sol. When used to form coatings, this method has been shown to yield films of greater thickness, density and quality than traditional sol–gel methods alone.[10–16]

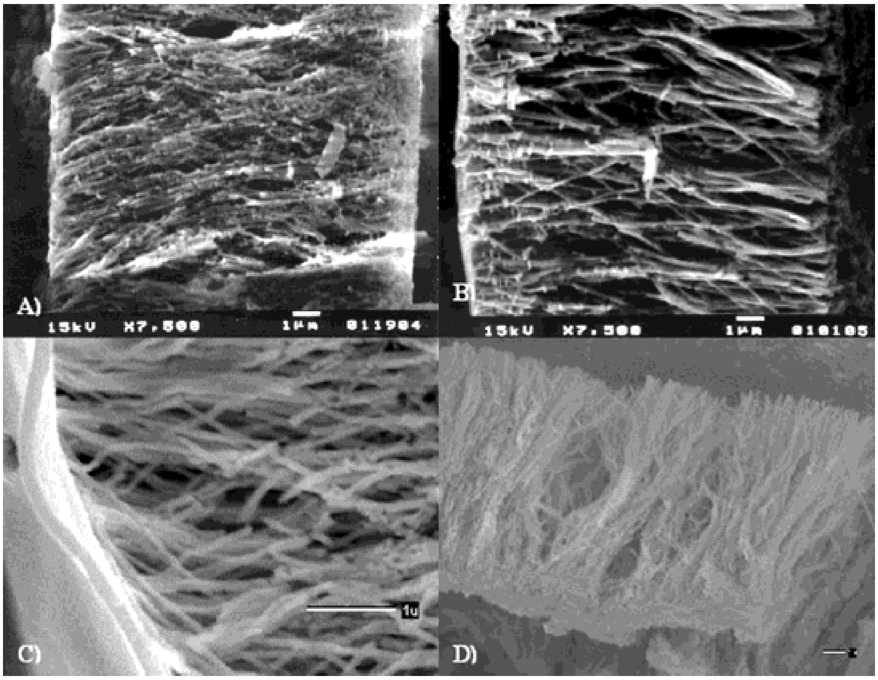

Fig. 1. a) PZT nanowires grown in a 100 nm diameter membrane. b) PZT nanowires grown in a 200 nm diameter membrane. c) Close up showing the films to which the nanowires are attached. d) Image showing the large area over which the wires are grown. The scale bar on all four images is 1 μm.

In this paper, we describe the use of sol–gel electrophoresis in the template-assisted growth of lead zirconate titanate (PZT) nanorods. Because of its ferroelectric and piezoelectric properties, PZT is a potentially important component of many systems, such as MEMS. As such, any method for producing PZT nanorods would be of great interest. In addition, we also believe that this technique should be adaptable to any oxide (single metal or complex) and organic–inorganic hybrids that can be synthesized by sol–gel methods. Details to the sol–gel electrophoresis of PZT are given in the experimental section.

Figure 1 shows SEM images of the PZT nanorods grown from the PZT sol by means of electrophoretic deposition and fired at 700–800 °C for 15–30 min in air. PZT nanorods grown in PC membranes with pore sizes of 100 and 200 nm show uniform size and near unidirectional alignment. The PZT nanorods have diameters smaller than that of the pores in the template membranes. The PZT nanorods have a size of approximately 70 nm when grown in a PC membrane with pores of 100 nm (Fig. 1a) and of 150 nm in a membrane with pores of 200 nm (Fig. 1b). The diameter difference of the grown nanorods and pores in the membranes could be attributed to the densification of nanorods when fired at 700–800 °C, which will be discussed further later in the paper. No PZT nanowires are observed from samples grown with 50 nm membranes. For the samples grown in 100 nm and 200 nm

0935-9648/01/1608-1270 $ 17.50+.50/0

membranes, it is seen that all the nanorods grew through the membrane from one side to the other, and that the length of the nanorods (~10 μm) resembled the thickness of the membranes. The PZT nanorods grown in both the 100 nm and 200 nm membranes show a uniform diameter throughout the entire length (Figs. 1a and b), with a surface that is smooth over much or all of the length. Furthermore, Figure 1b shows that a thin layer was formed at one end of the nanorods (left-hand side), which was exposed to the sol during the deposition. Such a thin PZT film is further demonstrated in Figure 1c. Figure 1d shows that PZT nanorods of uniform size and near-unidirectional alignment can be grown over a large area.

Figure 2 shows XRD spectra of the PZT nanorods and PZT powder prepared from the same sol; both PZT nanorods and powder consisted of only one crystalline phase, perovskite PZT without any detectable secondary phase. Comparison of the two spectra shows that there are identical peaks in both samples. Further, the peak positions are the same and the intensity ratios among various peaks are identical. The above XRD results indicate that the electrophoretic deposition has no detrimental influence on the stoichiometry and chemical compositional homogeneity that is achieved during the sol preparation. Furthermore, there is no preferred orientation of the crystals in the PZT nanorods.

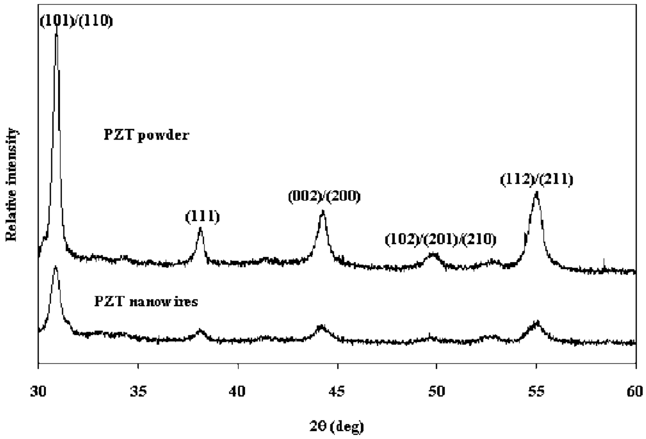

Fig. 2. XRD spectra of both the grown PZT nanowires and a powder derived from the same sol. Both samples show only a single perovskite phase, and there is no observed shift in the peak positions for the nanowire sample. In addition, the relative intensities of the peaks are the same for the nanowire sample, showing that there is no preferred orientation in the sample.

Sol–gel processing offers two advantages for the formation of complex oxide nanorods or nanorods. One of the advantages of sol–gel processing is that it allows molecular level chemical composition homogeneity. Appropriate sol preparation procedure yields solid nanoclusters with the desired stoichiometric chemical composition. These clusters are typically on the order of a few nanometers in size.[17] Another advantage of sol–gel processing is that solid nanoclusters will develop surface charge when dispersed in an electrolyte solvent, and are commonly stabilized by means of electrostatic double layers, which are formed by counter-ions surrounding the nanoclusters. Such charged nanoclusters will have an oriented diffusion when an electric field is applied to the system. In the present study, an electrophoretic deposition was applied to grow nanorods of PZT, capitalizing on the above advantages of sol–gel processing. Figure 3 is a schematic drawing of the electrophoretic deposition process. Under the experimental conditions applied in the current study, both the surface charge of the nanoclusters and the zeta-potential of the sol would be positive, since the pH of the sol (~4) is below the reported isoelectric point of PZT (~7.6),[18] and the sol concentration is low (~5 vol.-%). As such, the nanoclusters will be drawn towards the cathode and fill the pores of the membrane from the bottom of the pores, where is directly connected to the cathode. As the deposition proceeds, the electrical conduction between the cathode and the growth surface would be accomplished by the diffusion of counter-ions through the voids of packed nanoclusters. In this manner, all the pores will be completely filled. A thin layer of PZT could be formed on the membrane surface with prolonged deposition times. If we assume the nanoclusters are uniformly sized spheres, the highest packing density is 74 %,[19] which would be the highest achievable density of the nanorods before densification. When the nanorods are fired at elevated temperatures, densification would occur accompanied with shrinkage. The smaller diameter of nanorods relative to that of the membrane pores would be well explained by the shrinkage due to

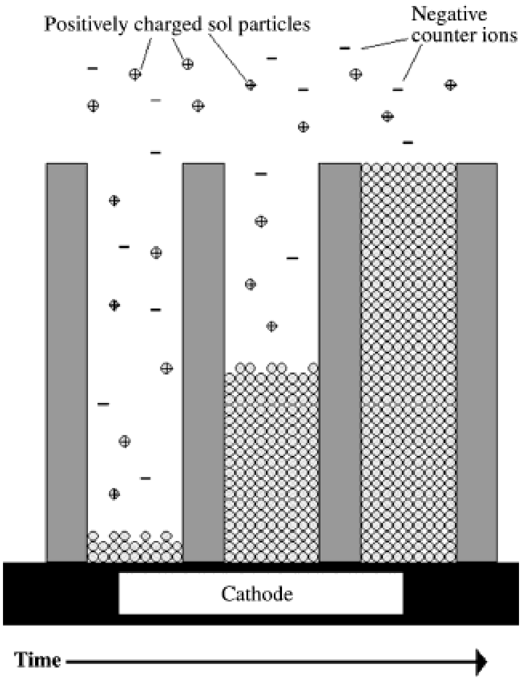

Fig. 3. This schematic demonstrates the progression of the growth process. At the left, we see the beginning of the nanowire growth. Positively charged sol particles are moving electrophoreticaly towards the negative electrode, depositing at the bottom of the pore, while the negatively charged counter ions are moving in the opposite direction. The center of the diagram shows a later time, as the densely packed sol particles fill up more of the pore. Lastly, the right side of the diagram shows a completely filled pore.

0935-9648/01/1608-1271 $ 17.50+.50/0

densification. A lateral shrinkage of approximately 25–30 % in diameter was observed when the nanorods were fired at 700–800 °C for 15–30 min. Although it is not known how closely the nanoclusters were packed during the electrophoretic deposition, since these times and temperatures are sufficient to fully densify PZT sol films, it is reasonable to assume that the nanorods are also fully dense after firing. This in turn implies that near ideal close packing might be achieved by this process.

The broken nanorods observed in Figure 1 could be explained as following. The PC membranes pyrolyze at approximately 400 °C in air, but the PZT nanorods are not fully dense or crystallized at this temperature, and thus have very limited mechanical strength. It is anticipated that some nanorods would break due to the different thermal expansion coefficient and distortion of PC membranes when they are heated to elevated temperatures and pyrolyzed. This also explains why some of the rods are slightly bent or curved. Since the PC membrane is not a perfectly rigid support, but distorts upon heating, some of the (not yet fully dense) nanorods will distort with it. The cause of the rough morphology observed on portions of some of the nanorods is unknown. This rough morphology was observed on most of the 150 nm PZT wires (the left side of Fig. 1b), but only rarely in 70 nm PZT wires (compare Figs. 1a and c, for instance). It is possible that the membranes cause this morphology, and further testing is being done to determine this.

At this time, efforts to synthesize PZT nanorods in the 50 nm diameter pores have not been successful. This may be due to a size effect. In the pores of the 50 nm membrane, diffusion of clusters may be very slow, even with an applied electric field. Another possible reason is that the nanorods of <50 nm in diameter may not have the mechanical strength to survive heating and subsequent handling. Further attempts to grow 50 nm diameter nanorods are underway.

In summary, we have demonstrated a new technique for the creation of complex oxide nanorods, specifically, PZT nanorods, using sol–gel electrophoresis. PZT nanorods with a diameter of 70–150 nm and a length of 10 μm were grown in PC membranes. This technique offers the advantages of growing large areas of uniformly sized and near unidirectionally aligned nanorods of complex oxide. It is also anticipated that nanorods with an aspect ratio far greater than 100 would be readily achievable. Desired stoichiometric chemical composition is readily obtained when an appropriate sol preparation procedure is used, whereas a post-deposition annealing at elevated temperatures is required to crystallize and densify the nanorods.

Experimental

For the formation of the PZT sol, the chemicals used were lead(II) acetate (99 %, Alfa Aesar, Ward Hill, MA), titanium(IV) isopropoxide (97 %, Alfa Aesar, Ward Hill, MA), zirconium *n*-propoxide (70 % in propanol, Alfa Aesar, Ward Hill, MA), glacial acetic acid (Fisher Scientific, Fair Lawn, NJ), lactic acid (Sigma Chemical, St. Louis, MO), ethylene glycol, and glycerol (both J. T. Baker, Phillibsburg, NJ). The template membranes used for the growth of PZT nanorods were track-etched hydrophilic PC (Millipore, Bedford, MA), with pore diameters of 50, 100, and 200 nm, and a thickness of 10 μm. These membranes are formed by irradiating a polymer sheet with fragments from a nuclear fission reaction, creating damage tracks in the polymer. These tracks are then preferentially etched to give randomly distributed, cylindrical pores of roughly uniform size [3].

The PZT sol is made in the following manner. First lead(II) acetate is dissolved in glacial acetic acid, heating to 110 °C for ~15 min to dehydrate the lead acetate. The sample is then allowed to cool back to room temperature. Because of the volatility of PbO, an excess amount of lead (5 mol-%) is used in the fabrication of this sol. Then titanium(IV) isopropoxide and zirconium(IV) *n*-propoxide are mixed together for ~10 min at room temperature, and added to the lead solution once it has cooled to room temperature. Deionized water is then added to initiate and sustain hydrolysis and condensation reactions, and the sol is stirred for ~15 min at room temperature. Lastly, lactic acid, glycerol and ethylene glycol are added to adjust the viscosity and stability of the sol. Such prepared sols have a concentration of about 5 vol.-% PZT, and are stable for several weeks at room temperature.

For the growth, an anode of Pt mesh is immersed in the sol. The cathode used is aluminum, covered with the PC template. The PC membrane is attached to the cathode with a piece of double-sided conductive (carbon) tape, to provide a conductive path from the membrane to the cathode. The cathode is placed on top of and just in contact with the sol, and the sol is drawn into the membrane pores by capillary action. For the electrophoretic growth, a potential of 5 V is applied between the electrodes, and held for 1 h. At the end of the electrophoretic deposition, excess sol is blotted off the membrane, and the membrane is then transferred from the cathode to a clean piece of Si wafer. Samples thus prepared are dried at ~100 °C for several hours, then placed in an oven and heated to between 700–800 °C for 15–30 min, to both densify and crystallize the PZT nanorods, as well as to burn off the PC membranes. The nanorods were sputter-coated with a thin Au/Pd layer, prior to morphology analysis using scanning electron microscopy (SEM, JEOL JSM-5200 and JEOL 840A). X-ray diffraction (XRD, Phillips PW1830) is used to determine the crystal structure and the formation of PZT phase.

Received: February 12, 2001
Final version: April 24, 2001

---

[1] B.-J. Kim, S.-G. Oh, M.-G. Han, S.-S. Im, *Langmuir* **2000**, *16*, 5841.
[2] H. Fukushima, S. Seki, T. Nishikawa, H. Takiguchi, K. Tamada, K. Abe, R. Colorado, Jr., M. Graupe, O. E. Shmakova, T. R. Lee, *J. Phys. Chem. B* **2000**, *104*, 7417.
[3] J. C. Hulteen, C. R. Martin, *J. Mater. Chem.* **1997**, *7*, 1075.
[4] A. Huczko, *Appl. Phys. A* **2000**, *70*, 365.
[5] L. Piraux, S. Dubois, S. Demoustier-Champagne, *Nucl. Instrum. Methods Phys. Res. B* **1997**, *131*, 357.
[6] C. Schönenberger, B. M. I. Van der Zande, L. G. J. Fokkink, M. Henry, C. Schmid, M. Krüger, A. Bachtold, R. Huber, H. Birk, U. Staufer, *J. Phys. Chem. B* **1997**, *101*, 5497.
[7] B. B. Lakshmi, C. J. Patrissi, C. R. Martin, *Chem. Mater.* **1997**, *9*, 2544.
[8] Y. Li, G. S. Cheng, L. D. Zhang, *J. Mater. Res.* **2000**, *15*, 2305.
[9] V. M. Cepak, J. C. Hulteen, G. Che, K. B. Jirage, B. B. Lakshmi, E. R. Fisher, C. R. Martin, *J. Mater. Res.* **1998**, *13*, 3070.
[10] H. Hirashima, Y. Obu, T. Nagai, H. Imai, *Mater. Res. Soc. Symp. Proc.* **1994**, *346*, 95.
[11] L. Shaw, R. Abbaschian, *J. Am. Ceram. Soc.* **1995**, *78*, 3376.
[12] H. Nishimori, K. Hasegawa, M. Tatsumisago, T. Minami, *J. Sol–Gel Sci. Technol.* **1996**, *7*, 211.
[13] H. Nishimori, M. Tatsumisago, T. Minami, *J. Mater. Sci.* **1996**, *31*, 6529.
[14] K. Hasegawa, H. Nishimori, M. Tatsumisago, T. Minami, *J. Mater. Sci.* **1998**, *33*, 1095.
[15] K. Katagiri, K. Hasegawa, A. Matsuda, M. Tatsumisago, T. Minami, *J. Am. Ceram. Soc.* **1998**, *81*, 2501.
[16] K. Hasegawa, S. Kunugi, M. Tatsumisago, T. Minami, *J. Sol–Gel Sci. Technol.* **1999**, *15*, 243.
[17] C. J. Brinker, G. W. Scherer, *Sol–Gel Sciences*, Academic, San Diego, CA **1990**.
[18] K. Baba, O. Nishizato, A. Takamura, M. Katsube, *J. Ceram. Soc. Jpn.* **1993**, *101*, 1370.
[19] J. S. Reed, *Principles of Ceramic Processing*, Wiley, New York **1995**.